

Inhomogeneous superconducting states in two weakly linked superconducting ultrathin films

Gao-Wei Qiu¹ and Yi Zhou^{2,3,1,4,*}

¹*Kavli Institute for Theoretical Sciences, University of Chinese Academy of Sciences, Beijing 100190, China*

²*Beijing National Laboratory for Condensed Matter Physics & Institute of Physics, Chinese Academy of Sciences, Beijing 100190, China*

³*Songshan Lake Materials Laboratory, Dongguan, Guangdong 523808, China*

⁴*CAS Center for Excellence in Topological Quantum Computation, University of Chinese Academy of Sciences, Beijing 100190, China*



(Received 3 January 2022; revised 8 March 2022; accepted 8 March 2022; published 23 March 2022)

A sufficiently large parallel magnetic field will generate staggered supercurrent loops and a superfluid density wave in two weakly linked superconducting (SC) ultrathin films, resulting in an inhomogeneous Fulde-Ferrell-Larkin-Ovchinnikov (FFLO) state. The SC order parameter of such an FFLO state is characterized by Bloch wave functions, called the “Bloch SC state.” The staggered supercurrent loops form an array of Josephson vortex-antivortex pairs, instead of the usual Josephson vortex lattice. Enclosing a unit cell of the array, the London’s fluxoid is quantized as $\Phi' = \Phi_0 = hc/2e$, while the net orbital magnetization caused by the staggered supercurrent is zero. Meanwhile, a small parallel magnetic field gives rise to an Fulde-Ferrell (FF) state that has uniform superfluid density. The phase transition between the Bloch SC state and the FF state belongs to the universality class of two-dimensional commensurate-incommensurate transitions. An analytical solution in terms of Jacobian elliptic functions is found to be an excellent approximation to the Bloch SC order parameter.

DOI: [10.1103/PhysRevB.105.L100506](https://doi.org/10.1103/PhysRevB.105.L100506)

Inhomogeneous superconductivity that breaks translational symmetry spontaneously has been attracting growing attention from diverse fields in physics, ranging from condensed matter to high-energy physics [1]. Quintessential examples for such inhomogeneous superconductors include the well-known Fulde-Ferrell-Larkin-Ovchinnikov (FFLO) state [2,3] and its generalized version, the pair density wave (PDW) state [4]. The FFLO or PDW state is a superconducting state with a nonuniform superconducting (SC) order parameter. Such an inhomogeneous SC state was proposed as a mother state of other ordering states. For instance, the partial melting of the PDW can give rise to a charge density wave (CDW) order, a uniform charge- $4e$ SC order, and a loop current order. Moreover, the PDW is expected to host fantastic quasiparticle excitations as well as topological defects, such as in-gap Bogoliubov quasiparticles in an s -wave superconductor and a half-flux ($hc/4e$) vortex bound with a CDW dislocation [4].

Meanwhile, extensive research activities in condensed matter physics and material sciences have been devoted to superconducting thin films and layered superconductors over the past several decades [5–7]. Indeed, layered superconductors can be viewed as intrinsic superconductors with weak links, namely, adjacent superconducting layers couple each other via Josephson junctions [8–12]. Among these research objects, two-dimensional (2D) SC systems in the presence of an in-plane magnetic field [13–15] is of particular interest, on which the emergence of unconventional superconductivity due to the applied magnetic field and spin-orbit coupling effect was proposed [14–16]. It has been suggested that an inhomogeneous FFLO state can be induced by an in-plane magnetic field in bilayer transition metal dichalcogenides (TMDs) [17],

such as MoS₂ [18,19] and NbSe₂ [20]. Very recently, with the help of a quasiparticle interference (QPI) technique, the experimental observation of a segmented Fermi surface inside the superconducting energy gap was reported in Bi₂Te₃ thin films proximitized by the superconductor NbSe₂ and under an in-plane magnetic field, which indicates the existence of a PDW or FFLO state [21].

In this Letter, we study a model for two weakly coupled SC ultrathin films in an applied parallel magnetic field, which allows us to explore various PDW states. The model is gauge invariant and essentially equivalent to the Lawrence-Doniach model [22,23] in the double-layer limit.

Model. We consider two layers of superconducting ultrathin films in the presence of an applied parallel magnetic field. These two layers are weakly linked to each other such that the Josephson tunneling current can flow in the direction perpendicular to them. The thickness of each layer d is considerably small compared to the penetration depth λ and coherence length ξ of the superconductor, so that a diamagnetic current loop cannot be induced by the applied in-plane magnetic field within each layer.

Assuming the separation between the two layers is a , we set up the coordinate system as depicted in Fig. 1(a), on which the external magnetic field is along the y direction, i.e., $\mathbf{H} = H\hat{\mathbf{y}}$. The corresponding vector potential is given by $\mathbf{A} = Hz\hat{\mathbf{x}}$ in the Landau gauge choice. Thus, the system is described by a two-component gauge-invariant Ginzburg-Landau (GL) free-energy functional [24] as follows,

$$f[\psi_1(\mathbf{r}), \psi_2(\mathbf{r})] = f_n + \sum_{l=1,2} \left\{ \alpha |\psi_l(\mathbf{r})|^2 + \frac{\beta}{2} |\psi_l(\mathbf{r})|^4 + \frac{1}{2m^*} \left| \left(\frac{\hbar}{i} \nabla - \frac{e^*}{c} \mathbf{A}_l(\mathbf{r}) \right) \psi_l(\mathbf{r}) \right|^2 \right\} + g[\psi_1(\mathbf{r})^* \psi_2(\mathbf{r}) e^{i\frac{2\pi}{\Phi_0} \int_2^1 \mathbf{A} \cdot d\mathbf{s}} + \text{c.c.}]. \quad (1)$$

*yizhou@iphy.ac.cn

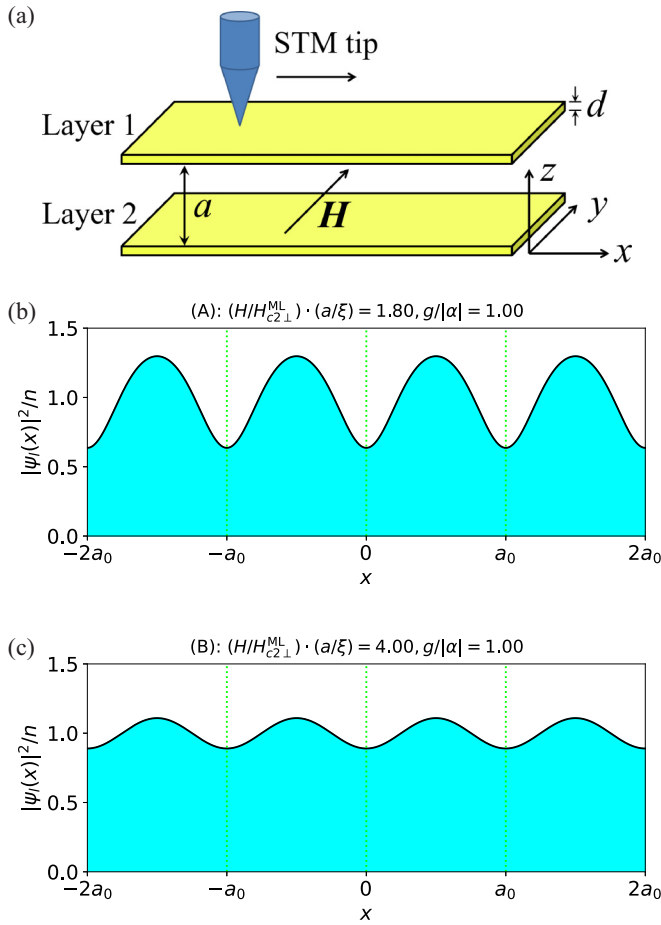


FIG. 1. (a) A bilayer SC system in an applied parallel magnetic field. The superfluid density wave can be probed by STM. Spatial modulation of the superfluid density for states (b) A and (c) B in the phase diagram (see Fig. 2).

Here, $l = 1, 2$ labels two layers, $\psi_1(\mathbf{r})$ and $\psi_2(\mathbf{r})$ are superconducting order parameters on them, and $\mathbf{r} = (x, y)$ is the 2D Cartesian coordinate. Since the thickness of each thin film $d \ll \lambda, \xi$, it is reasonable to presume that the order parameters are independent of z . Defining $\eta_1 = +1$ and $\eta_2 = -1$, the vector potential on each layer reads $\mathbf{A}_l(\mathbf{r}) = \eta_l(Ha/2)\hat{\mathbf{x}}$. The last term in Eq. (1) describes the Josephson tunneling effect, where g is the Josephson coupling energy. The orbital effect of the external magnetic field is introduced by the Peierls phase factor $e^{i\frac{2\pi}{\Phi_0} \int_2^1 \mathbf{A} \cdot d\mathbf{s}}$, which ensures the gauge invariance of the GL free energy. $\Phi_0 = hc/e^* = hc/2e$ is the flux quantum.

Note that our model is applicable to a superconductor-insulator-superconductor (S-I-S) junction, as long as the thickness of each superconducting layer $d \ll \lambda, \xi$. Such an S-I-S junction can be realized by the growth of a superconducting layer on both surfaces of an insulating thin film to form a sandwich structure. Other possible material realizations include but are not limited to superconducting TMDs.

The 2D model given in Eq. (1) can be further simplified. First, we consider the local tunneling between the two layers only, so that $\int_2^1 \mathbf{A} \cdot d\mathbf{s} = 0$ in the Landau gauge. Second, the Landau gauge choice gives rise to an explicitly y -independent form of GL free energy. Moreover, possible minima of the

GL free-energy functional are always given by $\partial_y \psi_{l=1,2} = 0$. Thus, the original 2D model can be simplified by the substitution $\psi_l(\mathbf{r}) \rightarrow \psi_l(x)$, and the GL free-energy functional will be reduced to the one-dimensional form as follows,

$$f[\psi_1, \psi_2] = f_n + \sum_{l=1,2} \left\{ \alpha |\psi_l|^2 + \frac{\beta}{2} |\psi_l|^4 + \frac{\hbar^2}{2m^*} \left| \left(\frac{\partial}{\partial x} - i\eta_l \frac{k_0}{2} \right) \psi_l \right|^2 \right\} + g(\psi_1^* \psi_2 + \psi_2^* \psi_1), \quad (2)$$

where a magnetic field-dependent wave vector $k_0 = 2\pi Ha/\Phi_0$ is introduced, and the corresponding length scale reads $a_0 = 2\pi/k_0 = \Phi_0/Ha$. The convenience of these notations will be seen later. Taking variations with respect to ψ_l^* in Eq. (2), we obtain coupled GL equations,

$$\alpha \psi_l + \beta |\psi_l|^2 \psi_l - \frac{\hbar^2}{2m^*} \left(\frac{\partial}{\partial x} - i\eta_l \frac{k_0}{2} \right)^2 \psi_l + g\psi_{\bar{l}} = 0, \quad (3)$$

where $l, \bar{l} = 1, 2$, and \bar{l} represents the opposite layer to l .

Symmetry. First of all, let us discuss relevant symmetry operations acting on coupled GL equations. The time reversal \mathcal{T} acts as $H \rightarrow -H$, $\psi_l(x) \rightarrow \psi_l(x)^*$, the spatial reflection \mathcal{P}_z acts as $l \rightarrow \bar{l}$, so that the joint operation \mathcal{TP}_z acts as $\psi_l(x) \rightarrow \psi_{\bar{l}}(x)^*$. It is remarkable that Eqs. (3) keep invariant under the operation \mathcal{TP}_z followed by the complex conjugate, thereby allowing a \mathcal{TP}_z symmetric solution, $\psi_{\bar{l}}(x)^* = \psi_l(x)$.

We begin with some exact solutions to Eqs. (3). It is easy to see that the coupled GL equations (3) have a trivial but exact solution, which is a Fulde-Ferrell (FF) state [2] indeed. Meanwhile, Eqs. (3) will become decoupled at $g = 0$, and give rise to another exact solution, called the decoupled SC state. Below we shall examine these two solutions:

(i) FF state. This state is given by a pair of constant order parameters on two SC layers, which takes the form

$$\psi_l(x) = \sqrt{\rho_s^{\text{FF}}} e^{i\varphi_l}, \quad (4)$$

where $\rho_s^{\text{FF}} = -\beta^{-1}(\alpha + \epsilon_H - |g|)$, and $\epsilon_H = \hbar^2 k_0^2 / 8m^*$ is an energy associated with the magnetic field H . Such a ground state carries diamagnetic supercurrent flow, and by definition, it is an FF state [25]. The phase difference $\Delta\varphi \equiv \varphi_1 - \varphi_2$ is determined as follows: (1) $\Delta\varphi = \pi$ for $g > 0$ and (2) $\Delta\varphi = 0$ for $g < 0$. The free-energy density reads $\mathcal{F}_{\text{FF}} = -\beta^{-1}(\alpha + \epsilon_H - |g|)^2$. The non-negative constraint to the superfluid density ρ_s^{FF} requires an upper bound for the external magnetic field H ,

$$H_c^* = \frac{\Phi_0}{\pi a \xi} \left(1 + \frac{2m^* \xi}{\hbar^2} |g| \right)^{1/2}, \quad (5)$$

where the superconductor coherence length ξ is determined by the relation $|\alpha| = \hbar^2 (2m^* \xi^2)^{-1}$. A nonzero FF state solution is not allowed when H exceeds H_c^* .

(ii) Decoupled SC state. When $g = 0$, Eqs. (3) have a plane-wave solution as follows,

$$\psi_l(x) = \sqrt{\rho_{s0}} e^{i\eta_l \frac{k_0}{2} x}, \quad (6)$$

where $\rho_{s0} = -\alpha/\beta$. The free-energy density for this decoupled SC state is $\mathcal{F}_D = -\alpha^2/\beta$. The inequality $\mathcal{F}_D < \mathcal{F}_{FF}$ always holds as long as $g = 0$ and $H < H_c^*$. Therefore, the decoupled SC state is energetically favored over the FF state in the absence of the Josephson tunneling.

In the presence of the Josephson tunneling, say, $g \neq 0$, the situation will be complicated and more interesting. In this case, the nontrivial exact solution to the nonlinear GL equations (3) is not available in general. However, we can raise the following issue: Does a SC state exist that is more energetically favored than the decoupled SC state and the FF state? To address this issue, we shall examine the well-known Bloch wave function that is a natural generalization of the plane wave and has been exploited to solve the nonlinear Schrödinger equation in the context of cold atoms [26].

Bloch SC state. In order to pursue a lower-energy SC state, we consider a more generic solution which takes the Bloch form as follows,

$$\psi_l(x) = e^{i\eta_l \frac{k_0}{2} x} \tilde{\psi}_l(x), \quad (7)$$

where $\tilde{\psi}_l(x + a_0) = \tilde{\psi}_l(x)$ is a periodic function and $a_0 = 2\pi/k_0$ as defined before. Following Ref. [26], we shall minimize the GL free-energy functional (2) by expanding $\tilde{\psi}_l$ in terms of plane waves,

$$\tilde{\psi}_l(x) = \sqrt{n} \sum_{v=-\infty}^{\infty} a_{lv} e^{ivk_0 x}. \quad (8)$$

where v is an integer, and $n = a_0^{-1} \int_0^{a_0} dx |\tilde{\psi}_l(x)|^2$ is the average superfluid density on each layer. The coefficients a_{lv} are subject to the normalization relation $\sum_{v=-\infty}^{\infty} |a_{lv}|^2 = 1$. Such a Bloch SC state will become the decoupled SC state when $a_{lv} = \delta_{v,0}$. Evaluating the GL free energy and minimizing it with respect to a_{lv} and n result in self-consistent equations as follows [27],

$$0 = \left(\frac{\hbar^2 k_0^2}{2m^*} v^2 + \alpha \right) a_{lv} + g a_{l, v+\eta_l} + n\beta \sum_{v_1, v_2} a_{lv_1}^* a_{lv_2} a_{l, v+v_1-v_2}, \quad (9a)$$

$$n = - \frac{\sum_{l=1,2} \left[\sum_v \left(\frac{\hbar^2 k_0^2}{2m^*} v^2 + \alpha \right) |a_{lv}|^2 + g \sum_v a_{lv}^* a_{l, v+\eta_l} \right]}{\beta \sum_{l=1,2} \sum_{v_1, v_2, v_3} a_{lv_1}^* a_{lv_2}^* a_{lv_3} a_{l, v_1+v_2-v_3}}. \quad (9b)$$

Note that Eqs. (9) can be derived from Eqs. (3) as well.

Before proceeding, we would like to make general remarks on the solutions to nonlinear equations (9): (1) It is more convenient to solve $\{n\beta, a_{1v}, a_{2v}\}$ instead of $\{n, a_{1v}, a_{2v}\}$, such that the parameter β will be irrelevant to the solutions. (2) Without loss of generality, we can set $|\alpha|$ as the energy unit, then the solution $\{n\beta, a_{1v}, a_{2v}\}$ will be determined by two independent parameters $g/|\alpha|$ and H . (3) For any solution, apart from an overall phase factor, the phase of $a_{lv} = |a_{lv}| e^{i\phi_{lv}}$ can be taken to be 0 or π [28]. (4) To solve Eqs. (9) numerically, the truncation of the series $\{a_{1v}\}$ and $\{a_{2v}\}$ has to be introduced, namely, $a_{1v} = a_{2v} = 0$ for $|v| > v_{\max}$, where v_{\max} is a positive integer. (5) The aforementioned $\mathcal{N}\mathcal{P}_z$ symmetry, $\psi_l(x)^* = \psi_l(x)$, is respected by all the numerically found solutions.

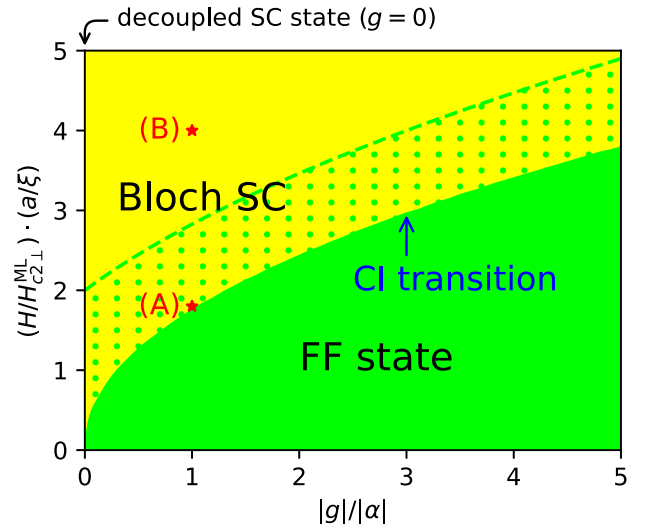


FIG. 2. Phase diagram. The Bloch SC state restores the decoupled SC state along the line of $g = 0$. The green dashed line in Fig. 2 indicates the upper bound H_c^* given in Eq. (5). The green dotted zone allows an FF state solution to exist, while it has higher free energy than the Bloch SC state. A commensurate-incommensurate (CI) transition occurs at the phase boundary between the Bloch SC state and the FF state. Two red stars mark Bloch SC states (A) and (B) at $|g|/|\alpha| = 1.0$ and A: $(H/H_{c2\perp}^{ML})(a/\xi) = 1.8$ and B: $(H/H_{c2\perp}^{ML})(a/\xi) = 4.0$, respectively.

Phase diagram. As discussed above, for a given set of independent parameters $(g/|\alpha|, H)$, Eqs. (9) can be solved numerically and the corresponding free-energy density $\mathcal{F}_{\text{Bloch}}$ can be computed subsequently. By comparing $\mathcal{F}_{\text{Bloch}}$ with the free-energy density of the decoupled SC state and the FF state, say, \mathcal{F}_D and \mathcal{F}_{FF} , we are able to obtain a phase diagram consisting of a decoupled SC state, FF state, and Bloch SC state, as shown in Fig. 2. Notice that if $\{n\beta, a_{1v}, a_{2v}\}$ is a solution to Eqs. (9) for a given pair of $(g/|\alpha|, H)$, then $\{n\beta, e^{i\pi v} a_{1v}, e^{i\pi v} a_{2v}\}$ will be a physically equivalent solution for $(-g/|\alpha|, H)$, so that the phase diagram can be parametrized by $(|g|/|\alpha|, H)$. Furthermore, H can be replaced by a dimensionless ratio $(H/H_{c2\perp}^{ML})(a/\xi)$. Here, $H_{c2\perp}^{ML} = \Phi_0(2\pi\xi^2)^{-1}$ is the perpendicular upper critical field of a monolayer SC thin film.

As seen in Fig. 2, a larger Josephson coupling energy $|g|$ and smaller applied parallel field H favor the FF state, while Bloch SC states will gain more free energy at smaller $|g|$ and larger H . As $|g|$ decreases and/or H increases, the energy cost in the kinetic term in Eq. (2) will be canceled by the phase factor $e^{i\eta_l k_0 x/2}$ in Eq. (7), resulting in $(\partial_x |\tilde{\psi}_l|)^2 \rightarrow 0$ and a more and more spatially uniform distribution of the superfluid density $|\psi_l(x)|^2$ [see Figs. 1(b) and 1(c)]. Along the line of $g = 0$, the Bloch SC state restores to the decoupled SC state given in Eq. (6) by taking a constant $\tilde{\psi}_l = \sqrt{\rho_{s0}}$ in Eq. (7). The green dashed line in Fig. 2 indicates the H_c^* given by Eq. (5), below which an FF state solution exists but has a higher free energy than the Bloch SC state in the green dotted zone, until H decreases further and enters the FF phase marked by the green zone.

It is noted that although the Bloch solution exists mathematically throughout the whole phase diagram, an actual parallel critical field $H_{c\parallel}$ will be determined physically by the parallel critical field for a monolayer thin film $H_{c\parallel}^{\text{ML}} = 2\sqrt{3}H_{c2\perp}^{\text{ML}}(\xi/d)$ [29] and/or the Pauli paramagnetic limit H_p [30,31], where d is the thickness of the thin film. The Bloch SC state will vanish when $H > H_{c\parallel}$.

Phase transition. The phase transition between the Bloch SC phase and the FF phase, which can be viewed as the melting of the superfluid density wave, turns out to be of the universality class of the commensurate-incommensurate (CI) transition, and is a second-order transition [32,33]. The effective model for such a transition can be written in terms of the relative phase $\phi(\mathbf{r})$ between the two layers [27],

$$H_{\text{eff}} = \rho_s \int d^2\mathbf{r} \left\{ \frac{\hbar^2}{2m^*} |\nabla\phi(\mathbf{r})|^2 + 2g \cos[\phi(\mathbf{r}) - k_0x] \right\}. \quad (10)$$

This is exactly the Pokrovsky-Talapov (PT) model in the context of incommensurate crystals [34], which was adopted to study double-layer quantum Hall systems [35,36]. In our case, the FF state corresponds to the commensurate state in the PT model, while the Bloch SC state corresponds to the incommensurate state that breaks the translational symmetry.

Spatial modulation of superfluid density. As mentioned, the \mathcal{TP}_z symmetry, $\psi_1(x) = \psi_2(x)^*$, is respected by all the found solutions. Consequently, the two layers have the same local superfluid density $|\psi_l(x)|^2$. For a Bloch SC state, as illustrated in Figs. 1(b) and 1(c), the superfluid density is modulated spatially by the applied magnetic field and manifests a PDW in each layer. Since the local superfluid density is associated with a local superconducting gap, this type of PDW can be probed by a scanning tunneling microscope (STM) [see Fig. 1(a)]. It is found that the spatial modulation will be enhanced when a Bloch SC state approaches the phase boundary (see the two states A and B in Fig. 2).

Supercurrent and Josephson tunneling effect. Now we proceed to study the intralayer supercurrent and interlayer Josephson tunneling current. The supercurrent density on each layer reads $\mathbf{J}_{sl} = \frac{e^*\hbar}{2m^*i}(\psi_l^*\nabla\psi_l - \psi_l\nabla\psi_l^*) - \frac{e^*}{m^*c}\psi_l^*\psi_l\mathbf{A}_l$ [29], which is in the direction perpendicular to the applied magnetic field H and can be written as $\mathbf{J}_{sl} = J_{sl}(x)\hat{x}$. On the other hand, the Josephson tunneling effect is characterized by the tunneling current density $J_T(x) = -\frac{e^*a}{\hbar}g \text{Im}(\psi_1\psi_2^*e^{i\frac{2\pi}{a_0}\int_1^2\mathbf{A}\cdot d\mathbf{s}})$.

For the Bloch SC state given by Eqs. (7) and (8), straightforward algebra leads to

$$J_{sl} = n \frac{e^*2Ha}{2m^*c} \sum_{vv'} 2va_{1v}a_{1v'} \cos[(v - v')k_0x], \quad (11a)$$

and

$$J_T = -n \frac{e^*a}{\hbar}g \sum_{vv'} a_{1v}a_{2v'} \sin[(v - v' + 1)k_0x]. \quad (11b)$$

Here, the fact that a_{1v} are real numbers has been used. Note that both J_{sl} and J_T are periodic, namely, $J_{sl}(x + a_0) = J_{sl}(x)$ and $J_T(x + a_0) = J_T(x)$. Moreover, owing to the \mathcal{TP}_z symmetry, $\psi_l(x)^* = \psi_l(x)$, we have $J_{sl}(x) = -J_{sl}(x)$, i.e., the local supercurrent flows in opposite directions on the two layers.

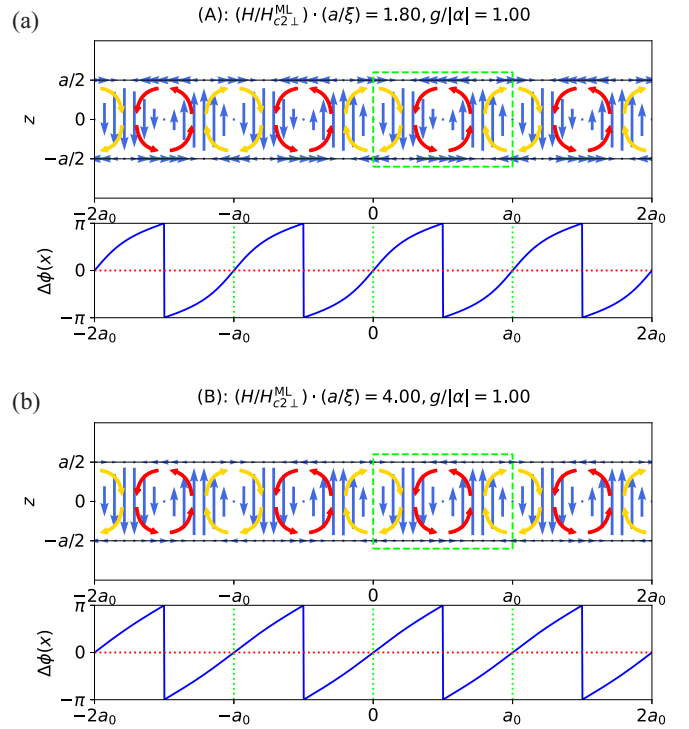


FIG. 3. The pattern of supercurrent and tunneling current (blue arrows), and the phase difference between the two layers. (a) Bloch SC state A in Fig. 2. (b) Bloch SC state B in Fig. 2. Red and yellow arrows indicate Josephson vortices and antivortices. Along each green dashed loop, a London's fluxoid can be defined, which is quantized as $\Phi' = \Phi_0$.

As examples, two typical Bloch solutions have been found numerically at $|g|/|\alpha| = 1.0$ and $(H/H_{c2\perp}^{\text{ML}})(a/\xi) = 1.8$ and 4.0 , respectively, which correspond to two points marked by red stars (A and B) in the phase diagram in Fig. 2. The supercurrent density and the tunneling current density are plotted in Fig. 3. These staggered currents form Josephson vortices and antivortices, as indicated by the red and yellow arrows in Fig. 3. It is remarkable that this array of Josephson vortex-antivortex pairs is different from the Josephson vortex lattice in the literature [37–39], although both are induced by a parallel magnetic field. The orbital magnetization generated by these currents is staggered, and the net orbital magnetization will vanish. This can be revealed by the London's fluxoid.

Fluxoid quantization. Considering a loop enclosing a period of a_0 (see the green dashed loops in Fig. 3), the London's fluxoid is defined as $\Phi' = \Phi + \frac{m^*c}{e^*2} \oint \frac{\mathbf{J}_s}{\rho_s} \cdot d\mathbf{s}$, where $\Phi = \oint \mathbf{A} \cdot d\mathbf{s} = Haa_0 = \Phi_0$ is the ordinary flux. For a Bloch SC state, we have $J_T(x + a_0) = J_T(x)$, and the second part in the fluxoid reads $\frac{m^*c}{e^*2} \oint \frac{\mathbf{J}_s}{\rho_s} \cdot d\mathbf{s} = \frac{\Phi_0}{2\pi} \oint \nabla\phi \cdot d\mathbf{s} - \oint \mathbf{A} \cdot d\mathbf{s}$. Therefore, $\Phi' = \Phi_0$ is exact the flux quantum, and the net orbital magnetization is counted by the flux $\frac{m^*c}{e^*2} \oint \frac{\mathbf{J}_s}{\rho_s} \cdot d\mathbf{s} = 0$ and vanishes.

In contrast, an FF state has uniform supercurrents $J_{sl}^{\text{FF}} = -\eta_l(e^*2Ha/2m^*c)\rho_s^{\text{FF}}$, which flow in opposite directions on the two layers and are perpendicular to the applied magnetic field. Meanwhile, the Josephson tunneling current vanishes, i.e., $J_T^{\text{FF}} \propto -g \sin(\Delta\phi) = 0$, because the phase difference between the two layers is $\Delta\phi = 0$ or π . Thus, for an FF state,

$\frac{m^*c}{e^2} \oint \frac{\mathbf{J}_s}{\rho_s} \cdot d\mathbf{s} = -\Phi_0$ and $\Phi' = 0$, suggesting perfect diamagnetism.

Approximate analytical solutions. It is remarkable that the Bloch SC state can be well approximated by the Jacobian elliptic functions cn and sn . When $g = 0$, Eqs. (3) reduce to two decoupled nonlinear Schrödinger equations, and each of them possesses exact periodic instanton solutions in the form of Jacobian elliptic functions [40,41]. While exact solutions are not available at a finite Josephson coupling g , we would like to propose approximate solutions as follows,

$$\psi_l(x) = [\mu \text{cn}(ux; r) + i\eta_l \text{vsn}(ux; r)]e^{i\varphi_l}, \quad (12)$$

where $\varphi_1 = \varphi_2 = 0$ for $g > 0$ and $\varphi_1 = -\varphi_2 = -\pi/2$ for $g < 0$. Here, $r \in (0, 1)$ is the modulus of the elliptic integral $K(r)$ [42], u is determined by the period through $4K(r) = 2ua_0$, and μ and ν are two constants and can be treated as variational parameters, which can be obtained by substituting Eq. (12) into Eq. (2) and minimizing the free energy with respect to μ , ν , and r . As examples, the optimization for the two states A and B in Fig. 2 gives rise to $r = 0.6023(90)$ and $r = 0.0559(55)$ for A and B, respectively.

By comparing the optimized solution given in Eq. (12) with that solved from Eqs. (9), we found that these two agree with each other with amazingly high precision. In a wide range of parameters ($g/|\alpha|, H$), the difference between the corresponding free energies is less than 0.01% [27].

Summary and discussions. In summary, we have found that two weakly linked SC ultrathin films in an applied parallel magnetic field H_{\parallel} can harbor various FFLO or PDW states, including the usual FF state and the proposed Bloch SC state. The latter is indeed a *superfluid density wave* state, and the spatial modulation of superfluid density can be verified by future STM experiments. The Bloch SC state is also characterized by its supercurrent pattern, which forms staggered loops. Thereby an array of Josephson vortex-antivortex pairs comes into being, instead of the usual Josephson vortex array. The phase transition between the FF state and the Bloch SC state is of second order, and can be described by the PT model [34].

Finally, the Bloch SC state is robust against an extra perpendicular magnetic field H_{\perp} . The problem of finding the upper critical magnetic field $H_{c2\perp}^{\text{BL}}$ in such a bilayer SC system can be mapped to the Rabi model in quantum optics [43], which can be solved numerically [44,45]. It turns out that there exists a finite $H_{c2\perp}^{\text{BL}}$, which is larger than the monolayer value $H_{c2\perp}^{\text{ML}}$ as long as the Josephson coupling g is nonzero [27].

Acknowledgments. We thank Dong-Hui Xu, Hong Yao, and Noah F. Q. Yuan for helpful discussions. In particular, we would like to thank Kun Yang for correcting the label of the FF state and bringing Refs. [34–36] to our attention. This work is partially supported by National Natural Science Foundation of China (No. 12034004 and No. 11774306) and the Strategic Priority Research Program of Chinese Academy of Sciences (No. XDB28000000).

-
- [1] R. Casalbuoni and G. Nardulli, *Rev. Mod. Phys.* **76**, 263 (2004).
 [2] P. Fulde and R. A. Ferrell, *Phys. Rev.* **135**, A550 (1964).
 [3] A. I. Larkin and Y. N. Ovchinnikov, *Zh. Eksp. Teor. Fiz.* **47**, 1136 (1964) [*Sov. Phys. JETP* **20**, 762 (1965)].
 [4] D. F. Agterberg, J. S. Davis, S. D. Edkins, E. Fradkin, D. J. Van Harlingen, S. A. Kivelson, P. A. Lee, L. Radzihovsky, J. M. Tranquada, and Y. Wang, *Annu. Rev. Condens. Matter Phys.* **11**, 231 (2020).
 [5] D. Eom, S. Qin, M.-Y. Chou, and C. K. Shih, *Phys. Rev. Lett.* **96**, 027005 (2006).
 [6] T. Morshedloo, M. Roknabadi, and M. Behdani, *Phys. C: Supercond. Appl.* **509**, 1 (2015).
 [7] L. N. Bulaevskii, *Sov. Phys. Usp.* **18**, 514 (1975).
 [8] B. D. Josephson, *Phys. Lett.* **1**, 251 (1962).
 [9] B. D. Josephson, *Adv. Phys.* **14**, 419 (1965).
 [10] K. K. Likharev, *Rev. Mod. Phys.* **51**, 101 (1979).
 [11] R. Kleiner, F. Steinmeyer, G. Kunkel, and P. Müller, *Phys. Rev. Lett.* **68**, 2394 (1992).
 [12] R. Kleiner and P. Müller, *Phys. Rev. B* **49**, 1327 (1994).
 [13] D. Agterberg, *Phys. C: Supercond. Appl.* **387**, 13 (2003).
 [14] V. Barzykin and L. P. Gor'kov, *Phys. Rev. Lett.* **89**, 227002 (2002).
 [15] K. Aoyama and M. Sigrist, *Phys. Rev. Lett.* **109**, 237007 (2012).
 [16] O. V. Dimitrova and M. V. Feigel'man, *J. Exp. Theor. Phys. Lett.* **78**, 637 (2003).
 [17] C.-X. Liu, *Phys. Rev. Lett.* **118**, 087001 (2017).
 [18] J. M. Lu, O. Zheliuk, I. Leermakers, N. F. Q. Yuan, U. Zeitler, K. T. Law, and J. T. Ye, *Science* **350**, 1353 (2015).
 [19] Y. Saito, Y. Nakamura, M. S. Bahramy, Y. Kohama, J. Ye, Y. Kasahara, Y. Nakagawa, M. Onga, M. Tokunaga, T. Nojima, Y. Yanase, and Y. Iwasa, *Nat. Phys.* **12**, 144 (2016).
 [20] X. Xi, Z. Wang, W. Zhao, J.-H. Park, K. T. Law, H. Berger, L. Forró, J. Shan, and K. F. Mak, *Nat. Phys.* **12**, 139 (2016).
 [21] Z. Zhu, M. Papaj, X.-A. Nie, H.-K. Xu, Y.-S. Gu, X. Yang, D. Guan, S. Wang, Y. Li, C. Liu, J. Luo, Z.-A. Xu, H. Zheng, L. Fu, and J.-F. Jia, *Science* **374**, 1381 (2021).
 [22] W. E. Lawrence and S. Doniach, in *Proceedings of the 12th International Conference on Low Temperature Physics*, edited by E. Kanda (Academic, Kyoto, 1971), p. 361.
 [23] K. Yang and S. L. Sondhi, *J. Appl. Phys.* **87**, 5549 (2000).
 [24] V. L. Ginzburg and L. D. Landau, *Zh. Eksp. Teor. Fiz.* **20**, 1064 (1950).
 [25] At first sight, the SC order parameter $\psi_l(x)$ does not vary spatially and suggests a uniform state rather than an FF state, which is true in the absence of a magnetic field. However, the situation changes in the presence of a magnetic field, because the SC order parameter does depend on the gauge choice and we should consider the gauge invariant physical observable, say, the current, instead. Indeed, this state carries finite and opposite supercurrents in both layers, so that it is an FF state by definition.
 [26] M. Machholm, C. J. Pethick, and H. Smith, *Phys. Rev. A* **67**, 053613 (2003).
 [27] See Supplemental Material at <http://link.aps.org/supplemental/10.1103/PhysRevB.105.L100506> for more details on numerical solution for Bloch SC states, analytical approximation, effective

- model near the commensurate-incommensurate phase transition, and the stability of this bilayer SC system against an extra perpendicular magnetic field.
- [28] Because $\phi_{l\nu}$'s occur in a free-energy functional in the form of $\cos(\phi_{l_1\nu_1} - \phi_{l_2\nu_2})$ and $\cos(\phi_{l_1\nu_1} - \phi_{l_2\nu_2} + \phi_{l_3\nu_3} - \phi_{l_4\nu_4})$, and a saddle point will be achieved at $\cos(\phi_{l_1\nu_1} - \phi_{l_2\nu_2}) = \pm 1$ and $\cos(\phi_{l_1\nu_1} - \phi_{l_2\nu_2} + \phi_{l_3\nu_3} - \phi_{l_4\nu_4}) = \pm 1$ [26], we can always choose $a_{l\nu}$ as real numbers.
- [29] M. Tinkham, *Introduction to Superconductivity*, 2nd ed. (McGraw-Hill, New York, 1996).
- [30] B. S. Chandrasekhar, *Appl. Phys. Lett.* **1**, 7 (1962).
- [31] A. M. Clogston, *Phys. Rev. Lett.* **9**, 266 (1962).
- [32] P. Bak, *Rep. Prog. Phys.* **45**, 587 (1982).
- [33] In the mean-field level, the fact that the amplitude oscillations of the Bloch state increase as approaching the phase boundary indicates a first-order phase transition. However, this phase transition will become continuous when fluctuations are considered. Physically, around the critical point, the fluctuations are dominated by domain wall fluctuations, and the universality class has been determined and is known as the PT universality class (see Ref. [32] for more details).
- [34] V. L. Pokrovsky and A. L. Talapov, *Phys. Rev. Lett.* **42**, 65 (1979).
- [35] K. Yang, K. Moon, L. Zheng, A. H. MacDonald, S. M. Girvin, D. Yoshioka, and S.-C. Zhang, *Phys. Rev. Lett.* **72**, 732 (1994).
- [36] K. Yang, K. Moon, L. Belkhir, H. Mori, S. M. Girvin, A. H. MacDonald, L. Zheng, and D. Yoshioka, *Phys. Rev. B* **54**, 11644 (1996).
- [37] A. E. Koshelev and M. J. W. Dodgson, *J. Exp. Theor. Phys.* **117**, 449 (2013).
- [38] G. R. Berdiyrov, M. V. Milošević, F. Kusmartsev, F. M. Peeters, and S. Savel'ev, *Sci. Rep.* **8**, 2733 (2018).
- [39] P. J. Curran, H. A. Mohammed, S. J. Bending, A. E. Koshelev, Y. Tsuchiya, and T. Tamegai, *Sci. Rep.* **8**, 10914 (2018).
- [40] J.-Q. Liang and H. J. W. Müller-Kirsten, *Phys. Rev. D* **46**, 4685 (1992).
- [41] K. Funakubo, S. Otsuki, K. Takenaga, and F. Toyoda, *Prog. Theor. Phys.* **87**, 663 (1992).
- [42] The modulus r characterizes the shape of Jacobian elliptic functions, e.g., $\text{cn}(x; 0) = \cos(x)$, $\text{sn}(x; 0) = \sin(x)$ and $\text{cn}(x; 1) = \text{sech}(x)$, $\text{sn}(x; 1) = \tanh(x)$.
- [43] I. I. Rabi, *Phys. Rev.* **49**, 324 (1936).
- [44] D. Braak, *Phys. Rev. Lett.* **107**, 100401 (2011).
- [45] Q.-H. Chen, T. Liu, Y.-Y. Zhang, and K.-L. Wang, *Europhys. Lett.* **96**, 14003 (2011).